Mat. Res. Soc. Symp. Proc. Vol. 758 © 2003 Materials Research Society LL4.4

MTU Laser-Based Direct-Write Techniques: Recent Development and Nanoparticles Patterning Results

Edward M. Nadgorny[1], Changgong Zhou[1], Jaroslaw Drelich[2, 3], and Randy Zahn[2]
[1]Department of Physics, [2]Department of Materials Science and Engineering, and [3]Engineering Research Center for Wireless Integrated Microsystems, Michigan Technological University, 1400 Townsend Drive, Houghton, MI 49931, U.S.A.

ABSTRACT

Two laser-based direct-write techniques to guide particles from a mist source to a target substrate by laser beams were recently developed at Michigan Tech. The laser-guided direct-write (LGDW) technique uses a hollow optical fiber, while the laser-guided microsensor patterning (LGMP) technique uses a micrometer-sized aperture. The techniques are suggested to be utilized for patterning microstructures made of nanoparticles that are either crystallized from liquid precursors or directly deposited from nanoparticle-in-liquid suspensions. The computational results based on the paraxial Fraunhofer approximation of a Gaussian beam diffracted by a circular aperture and experimental measurements of corresponding deposition rate under different conditions suggest several factors for setup optimization of LGMP. The results indicate that among the most important factors are the aperture size relative to the laser beam-waist size and the divergence of the beam near the aperture. Examples of gold-thiolate, protein-coated polystyrene, and carbon-polymer composites deposition are presented.

INTRODUCTION

Laser-based guidance of nanoparticles is one of many techniques in the new emerging field of direct-write technologies allowing effective and advanced patterning of various materials for the fabrication of sensors and electronics (see an extensive review [1] for more details). Two laser-based techniques have recently been developed at MTU, LGDW and LGMP [2-6]. Both of the techniques use laser-induced optical forces to transport particles from a supply source and deposit them on a substrate mounted on a translation stage. They are differentiated mainly by the method of focusing the particles before depositing on the substrate: LGDW uses a hollow optical fiber while LGMP an aperture and lens-controlled narrow laser beam. These techniques are quite general and enable one to deposit almost any material that can be atomized to produce micron or submicron-sized carriers, i.e. liquid droplets. Such droplets may be in the form of liquid precursors, single-phase liquid solutions or colloidal suspensions of solid particles. Complex structures can be patterned by repeatedly depositing individual particles on the translated substrate. The techniques can operate over a wide range of particles sizes, from several nm to about one micron. So far, a variety of structures have been constructed on different substrates using metals, dielectrics, semiconductors, piezoelectric and ionic crystals, as well as living cells and proteins [2-7].

Unlike well-known optical trapping techniques, the laser-based direct-write techniques utilize optical transverse gradient forces to confine particles inside weakly focused laser beams and take advantage of radiation pressure and absorption force to move particles axially. An optical trap, on the other hand, sometimes referred to as an optical tweezer, see [8] for review, makes use of a strongly focused laser beam with a very strong axial gradient to allow axial trapping. This difference also illustrates the main advantage of the direct-write techniques over

optical tweezers: their ability to transport particles from various particle sources onto substrates to "write" on them. This paper briefly describes the setup and features of the MTU LGDW and LGMP techniques and shows some recent examples of their applications in deposition of nanomaterials.

MTU TECHNOLOGIES

The principal setup of the laser-based direct-write techniques is shown schematically in Figure 1. It consists of a mist chamber (MC), source chamber (SC), process chamber (PC), and a laser system. The mist chamber includes an atomizer and delivery system to make a mist of sub-micron sized liquid droplets that are precursors for the deposited material. The source chamber is connected to a process chamber by a micron-sized hollow optical fiber (LGDW) or aperture (LGMP). Typical fiber and aperture sizes are about 20 μm, and the droplets must be much smaller than the fiber or aperture sizes, typically being of the order of a micron or less. The laser beam is coupled into a fiber or aperture by an optical lens of low numerical aperture to allow particle guidance to a substrate that is mounted on a translational stage. The supply chamber provides an environment suitable for the deposition process and shields the particles from convection currents that can deflect particles out of laser's confinement. More details can be found in [2-4, 7] for LGDW and in [5, 6] for LGMP. The main difference between the two versions is that LGDW utilizes the guiding optical fields in a grazing-incidence mode inside the hollow fiber, while the guidance in LGMP is achieved by diffracted laser radiation.

As mentioned, the guidance efficiency depends strongly on the optical transverse gradient force and, therefore, on the optical axial intensity. The intensity inside a hollow fiber decreases exponentially with the distance, and the decay is usually characterized by a parameter z_0 or the decay length. For a typical fiber of the inner diameter $2a = 20$ μm, $z_0 \approx 8$ mm, and it is size and wavelength dependent, $z_0 \propto a^3/\lambda^2$ [3]. The equivalent circular-aperture parameter is the Rayleigh range z_R, or the border between the near-field diffraction region (at $z < z_R$) and the

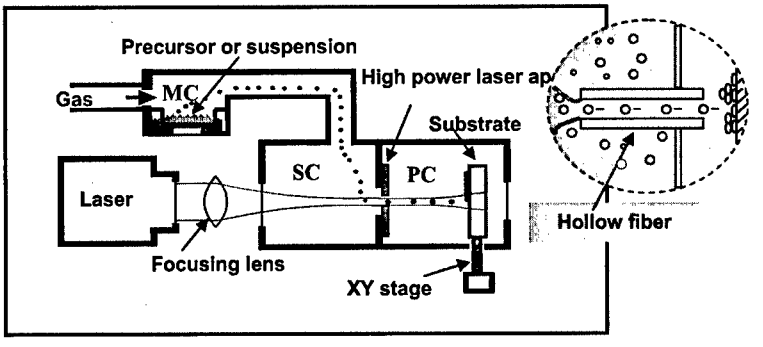

Figure 1. Schematic of laser-based direct-write techniques: source of droplets/particles (atomizer, carrier gas supply and the mist chamber MC); laser system (laser and focusing lens); supply (SC) and process (PC) chambers linked by either the high-power laser aperture (LGMP) or hollow optical fiber (LGDW, shown in the offset); movable substrate on a translational stage.

far-filed diffraction region (at $z > z_R$). The Rayleigh range scales approximately as $z_R \propto a^2/\lambda$, being typically shorter than z_0 [9]; for instance, $z_R \approx 1$ mm for the 25-μm aperture. Unlike the hollow fiber case, the intensity in the near-field region might be even higher than the incident light intensity, decreasing only at $z > z_0$. Additionally, LGMP practically excludes particles clogging and allows lower laser intensity; it also free from attenuation limits of LGDW due to smaller hollow fiber size. On the other hand, LGMP is more sensitive to axial gradient forces, especially for such nanoparticles as gold with a higher polarizability [10] and requires a better optical design to avoid the inverse radiation pressure.

The computational results based on the paraxial Fraunhofer approximation of a gaussian beam diffracted by a circular aperture [9, 11] suggest several factors for setup optimization of LGMP. The calculations and experimental comparison of the diffraction patterns with the best particle flux through the 25-μm aperture have shown that one of the most important factors is the aperture radius a relative to the gaussian beam-waist radius w_0. It was found that the ratio a/w_0 should be at least equal to or larger than 1.7. This number is larger than an optimum aperture ratio of 1.125 (to obtain the maximum axial intensity in the far-field range) but closer to 1.57 for ≥ 99% power transmission [12]. The other important factor is the divergence of the beam ahead of the aperture. A large divergence in the region near the beam waist (as utilized in the optical tweezers [8]) can lead to reverse radiation pressure, especially for small particles $<< \lambda$ [10]. Experiments with a setup (100-nm polystyrene spheres, 25-μm circular aperture and 30-mm focusing lens) have shown that guidance exists at as low laser power as ≤ 100 mW.

High accuracy is essential for direct write applications. Since it is determined by many factors, systematic studies are required to estimate their contributions. Preliminary experiments with five different materials [13] have shown that the deposition accuracy is inversely proportional to the transport distance; it also strongly depends on the material properties of the transported particles, such the refractive index and absorption, and relatively weakly on the laser power when measured inside a low-power range.

RESULTS AND DISCUSSION

All experiments discussed below were performed using a cw frequency doubled Nd:YVO_4 laser (Millennia II, Spectra-Physics, $\lambda = 532$ nm, 2.0 W, TEM_{00} mode) for deposition and an AFM (Dimension 3000) for characterization. Glass substrates were cleaned using a standard procedure (Alconox powder cleaner and ultrasonic bath). Some substrates were additionally silanized.

Deposition of gold-thiolate nanoparticles

Synthesis of new materials, including nanomaterials, can take advantage of the laser heating of droplets during their transportation and deposition. The techniques allow us in-situ melting of deposited gold particles to form microelectrodes at the ends of nanoparticle depositions; additionally, porous microstructures can result from evaporation of the deposited nanoparticle-in-liquid droplets [5, 6]. Porous and relatively uniform microstructures can be fabricated using as small nanoparticles as a few nm. Figure 2a shows spheres made of 7-nm hydrophobic gold particles. The size of these spheres varies from about 200 nm to one micron, and the diameter of the spheres is a direct consequence of the size distribution of the nanoparticle-in-liquid droplets

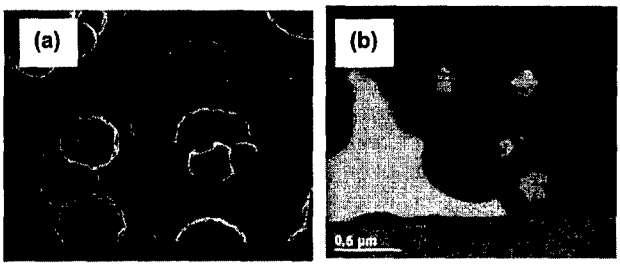

Figure 2. Structures formed by 7-nm Au-S$(CH_2)_7CH_3$ particles deposited by at a laser power of 200 mW on glass: (a) scanning electron micrograph of microspheres; (b) transmission electron micrograph of the partially sectioned microspheres.

generated by the atomizer and, to a lesser degree, the nanoparticle concentration in the droplets. The hydrophobic gold nanoparticles pack together producing stable microstructures as a result of the inter-particle van der Waals forces.

The transmission electron micrograph in Figure 2b reveals that the spheres are empty inside as indicated by a bright area of the sectioned spheres. Such an inhomogeneity reduces the strength of fabricated microstructures and causes a partial collapse of the shells. As a result, small undulations are formed, as can be seen in Figure 2a. The formation of such shells is assumed to be a result of combined effects of liquid evaporation and capillarity phenomena. Indeed, when the laser beam heats liquid droplets, evaporation progresses easily through the outer surface of the droplets. It is also initiated on the nanoparticle surfaces inside the droplets via nucleation and growth of nanobubbles. As long as the density of nanoparticles in the droplet is small, the bubbles can easily escape to the droplet surface. This is not the case, however, when a dense structure of nanoparticles is created producing fine porosity through particle-to-particle alignment. In this situation, a dense monolayer of hydrophobic gold nanoparticles has probably already been formed on the surface of each toluene droplet at an early stage of the fabrication experiment, soon after droplet generation. Gaseous bubbles cannot pass through such a dense configuration of nanoparticles without disrupting its structure due to high capillary pressure opposing this process. An estimate by the simplified Young-Laplace equation $\Delta P = 2\gamma / R$, where γ is the surface tension of liquid and R is the radius of capillary opening, shows that a pressure of about 280 atm is required to force the gaseous-toluene interface to move through a capillary opening of 4 nm in diameter.

It remains to be seen if the hollow microspheres made of gold and other nanoparticles synthesized in our laboratory can found new application, such as capsules for the controlled release of drugs and production of new catalysts with controlled porosity and specific surface area.

Deposition of polystyrene nanospheres

Spherical polystyrene nanoparticles are attractive for patterning due to their availability in a variety of sizes and their well-known surface properties. They are also commonly used as carriers for proteins in biosensor fabrication. When deposited from water suspensions, both polystyrene nanoparticles and polystyrene nanoparticles coated with avidin proteins form spherical well-ordered structures. Additionally, avidin proteins remain active on the surface of the carrier polystyrene particles after their deposition with LGMP [5]. Two examples of such cluster-like structures made of 100-nm protein-coated and uncoated polystyrene particles (Duke Scientific) by 200-mW power deposition are shown in Figure 3. Small irregularities of several nm in width were observed only on avidin-coated polystyrene. They are assumed to be formed due to incomplete coating of the polystyrene particles with protein layer(s). Proteins adsorb on the hydrophobic surface of polystyrene from solution and can also be deposited through the

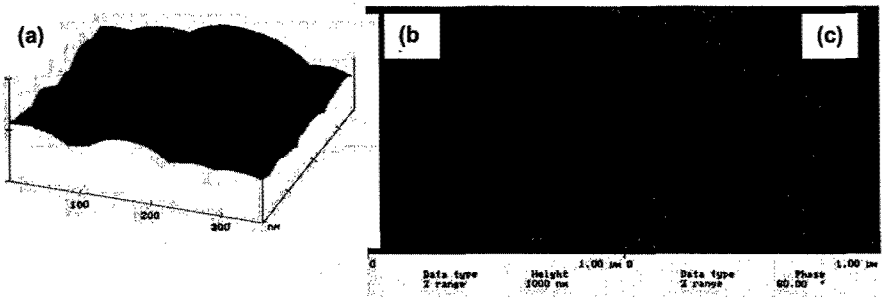

Figure 3. (a) AFM 3-D topographic image of clusters of 100-nm avidin-coated polystyrene particles deposited on silanized glass. (b) AFM topographic image of 100-nm uncoated polystyrene particles deposited on untreated glass. (c) AFM phase image of the same particles.

liquid-solid-air three-phase line during its retraction when the volume of liquid decreases.

As our experiments indicated, LGMP opens an option to control the size and the shape of the deposited clusters. At a higher evaporation rate (particles with strong absorption and/or a higher laser power), the deposited particles carry no or little water, forming spherical clusters similar to those shown in Figure 2. At a lower evaporation rate (particles with weak absorption and/or lower laser power), deposited droplets are still liquid and spread polystyrene spheres to form lens-like clusters, such as shown in Figure 3c. Thus, the shape and size of formed clusters can be controlled by changing the substrate wetting properties (hydrophilic/hydrophobic).

Deposition of carbon-polymer composite

The resistivity of polymers is commonly changed by incorporating conductive particles, such as carbon and metals, into the polymeric matrix. Such composites constitute an attractive basis for sensing devices based on the absorption of organic pollutants by the polymeric matrix. Contaminants absorption causes the polymer to swell, which increases the distance between conductive particles and changes the conductivity of the composites. Chemical stability of such composites combined with their good adhesion to many substrates are additional attractive features in patterning of this type of materials over many other systems of weakly interacting particles.

Fabrication of microstrips of carbon-polymer composites is currently explored in our research using LGMP. Commercially available carbon nanoparticles of irregular shape (from 30 to 100 nm) are suspended in polyvinyl acetate-toluene solutions for atomization and deposition. Our goal is to investigate the stability and controlled melting of such a composite under the laser beam, as well as the phase segregation inside the deposited matrix. As an example, Figure 4 shows a cluster of carbon-polyvinyl acetate deposited on glass. Carbon nanoparticles (300 mg) were dispersed in a solution of 3.2 g polyvinyl acetate in 50 ml toluene. Both AFM phase and 3-D images reveal locations of a few carbon particles on the surface of polymeric cluster visible as small dark and regular areas. They can also be distinguished from irregularities of the cluster surface of 3D topographic image. Note that the body of each carbon particle remains immersed in the polymeric matrix. The accumulation of carbon particles at the surface of a polymeric droplet is a rare phenomenon since the carbon particles have a tendency to remain dispersed in the polymeric matrix. This is the result of strong interactions between polyvinyl acetate and carbon particles used in this study.

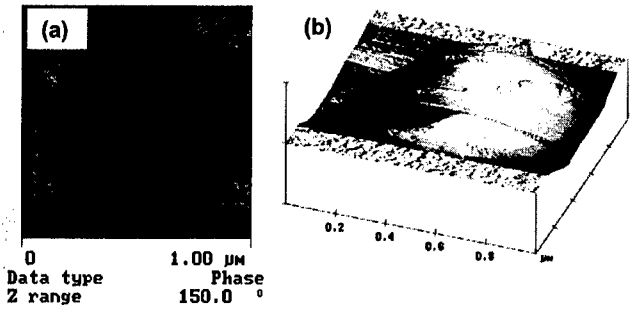

Figure 4. A cluster of carbon-polyvinyl acetate of about 1 µm in diameter and 0.5 µm in height deposited on glass at a laser power of 0.3 W: (a) AFM phase image; (b) AFM 3D topographic image.

ACKNOWLEDGEMENTS

The authors would like to express their appreciation to Elvin Beach and Steve Rozeveld of Dow Chemical Company for their help on scanning electron microscopy and transmission electron microscopy images and to Juntao Xu for deposition of gold-thiolate nanoparticles. The gold-thiolate nanoparticles were received from E.T. Zellers of the University of Michigan.

REFERENCES

1. A. Pique and D.B. Chrisey (editors), *Direct-Write Technologies for Rapid Prototyping Applications* (Academic Press, 2002).
2. M. J. Renn and R. Pastel, *J. Vac. Sci Technol.* **B16**, 3859 (1998).
3. M. J. Renn, R. Pastel, and H. J. Lewandowski, *Phys. Rev. Lett.* **82**, 1574 (1999).
4. E.M. Nadgorny, R.L. Pastel, A.A. Struthers, and A. Miner in *Mass and Charge Transport in Inorganic Materials - Fundamentals to Devices, Part B*, edited by P. Vincenzini and V. Buscaglia (Intl. Conf. Proceedings, Italy, Techna, Faenza, 2000), pp 1107-14.
5. J. Xu, Ch. Zhou, Sh. Grant, E. Nadgorny, and J. Drelich in *Functional Nanostructured Materials Through Multiscale Assembly and Novel Patterning Techniques* (Mater. Res. Soc. Proc. **728**, Pittsburgh, PA, 2002), pp. S7.6.1-6.6.
6. J. Drelich, E.M. Nadgorny, E.T. Zellers, J. Xu, Ch. Zhou, C.L. White, and W.M. Cross in *Functional Fillers and Nanoscale Minerals*, edited by J.J. Kellar, M.A. Herpfer, and B.M. Moudgil (Proc. of Intl Symp., SME, Littleton, OH, 2003), pp. 85-94.
7. M.J. Renn, G. Marquez, B.H. King, M. Essien, and W.D. Miller in [1], pp. 475-92.
8. A. Ashkin, *Optical Trapping and manipulation of neutral particles using lasers* (World Scientific, 2002).
9. A. Siegman, *Lasers* (University Science Book, 1986), p. 729.
10. K. Svoboda and S. M. Block, *Opt. Lett.* **19**, 930 (1994).
11. J.P. Campbell and L.G. DeShazer, *J.Opt. Soc. Am.* **59**, 1427 (1969).
12. Ref. [11], pp. 666 and 734.
13. R. Pastel, P. Geiser, A. Strutheres, E. Nadgorny (2000), unpublished results.